Polarity transitions induced by symmetry-breaking outer boundary heat flux in rapidly rotating dynamos

SUPPLEMENTARY MATERIAL

Debarshi Majumder and Binod Sreenivasan*

S1 The evolution of a dynamo from a seed magnetic field: The role of slow MAC waves in dipole formation

We consider a convection-driven dynamo operating in a spherical shell, the boundaries of which correspond to the inner core boundary and the coremantle boundary. The ratio of inner to outer radius is 0.35. Lengths are scaled by the thickness of the spherical shell L and time is scaled by magnetic diffusion time L^2/η. The velocity $\boldsymbol{u}$ and magnetic field $\boldsymbol{B}$ are scaled by η/L and $(2\Omega\rho\mu\eta)^{1/2}$, respectively. The temperature is scaled by βL, where β is the radial temperature gradient at the outer boundary. The non-dimensional MHD equations for the velocity, magnetic field and temperature are given in equations (3.1)–(3.4), §3. While η, ρ, μ and Ω above are defined in §2, the dimensionless parameters and the basic state buoyancy profile used in the dynamo model are described in §3. The velocity and magnetic fields satisfy the no-slip and electrically insulating conditions respectively at the two boundaries. The inner boundary is isothermal while the outer boundary has constant heat flux.

Figure S1 presents the evolution of the dynamo initiated from a seed magnetic field. The slow MAC waves onset at the point A, when the Alfvén wave and buoyancy wave frequencies are approximately equal, i.e. $|\omega_M| \approx |\omega_A|$. Point B denotes a multipolar state in which slow waves are present, while the dotted line at point C indicates the formation of the axial dipole. Figure S2 shows the relative magnitudes of the axial components of the curled Coriolis, buoyancy, and Lorentz forces at point 'B', where the slow MAC wave frequency ω_s is nonzero and yet the dynamo is in a multipolar state. Here, the Coriolis force is balanced by both the buoyancy and Lorentz forces at several points within the volume. The Lorentz force essentially consists of the non-dipolar part of the field since the dipole field has not formed and therefore has a negligible contribution (figures S2 d & e). Figure S3 shows the measurement of wave motion in the dynamo at time 'B'. Contours of $\partial u_z/\partial t$ at a cylindrical radius $s = 1$ for the energy-containing range of spherical harmonic degrees $l \leq l_E$ are plotted over short time windows during which the ambient magnetic field and wavenumbers remain approximately constant. At the instant 'B', both slow and fast MAC waves coexist. The slow MAC waves are generated at several points where the magnetic flux is concentrated so that localized balances between the Lorentz, Coriolis and buoyancy forces exist. The fast waves are present in regions where the magnetic flux is relatively weak. The measured and estimated axial group velocities of the waves at different points within the volume are shown in figure S2 (f). The method of their calculation is given in Varma & Sreenivasan (2022).

The helicity of the slow MAC waves generated from the non-dipolar magnetic flux is essential for formation of the axial dipole (see Varma & Sreenivasan, 2022; Majumder *et al.*, 2024). In the hydrodynamic dynamo at the same parameters where the Lorentz force is zero, the field stays multi-

*Email: bsreeni@iisc.ac.in

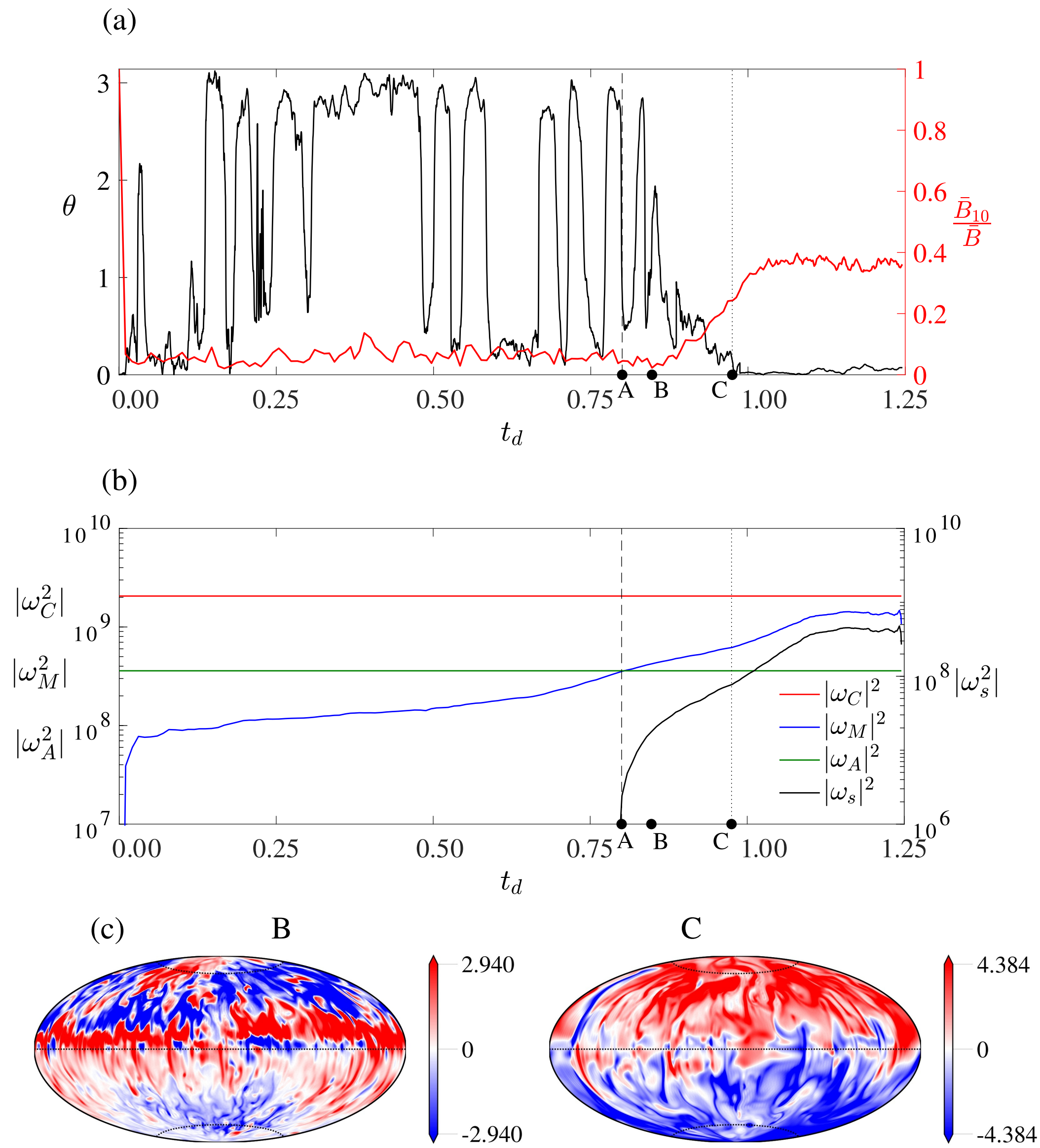

Figure S1: (a) Evolution of the dipole colatitude θ and the ratio of the root mean square values of the axial magnetic field ($\bar{B}_{10}$) to the the total magnetic field ($\bar{B}$) with time in units of the magnetic diffusion time. The simulation begins from a seed magnetic field. (b) The evolution in time of the fundamental frequencies. The vertical dashed line at point A indicates the emergence of slow MAC waves, which occurs when $|\omega_M| \approx |\omega_A|$, and the dotted line at point C indicates the time of dipole formation. Point B represents a multipolar state where slow waves are present. (c) The contours of radial magnetic field at the outer boundary is shown for points ‘B’ and ’C’. The dynamo parameters are as follows: Ekman number $E = 1.2 \times 10^{-5}$, modified Rayleigh number $Ra = 5000$, Prandtl number $Pr = 1$ and magnetic Prandtl number $Pm = 1$. See also Varma & Sreenivasan (2022).

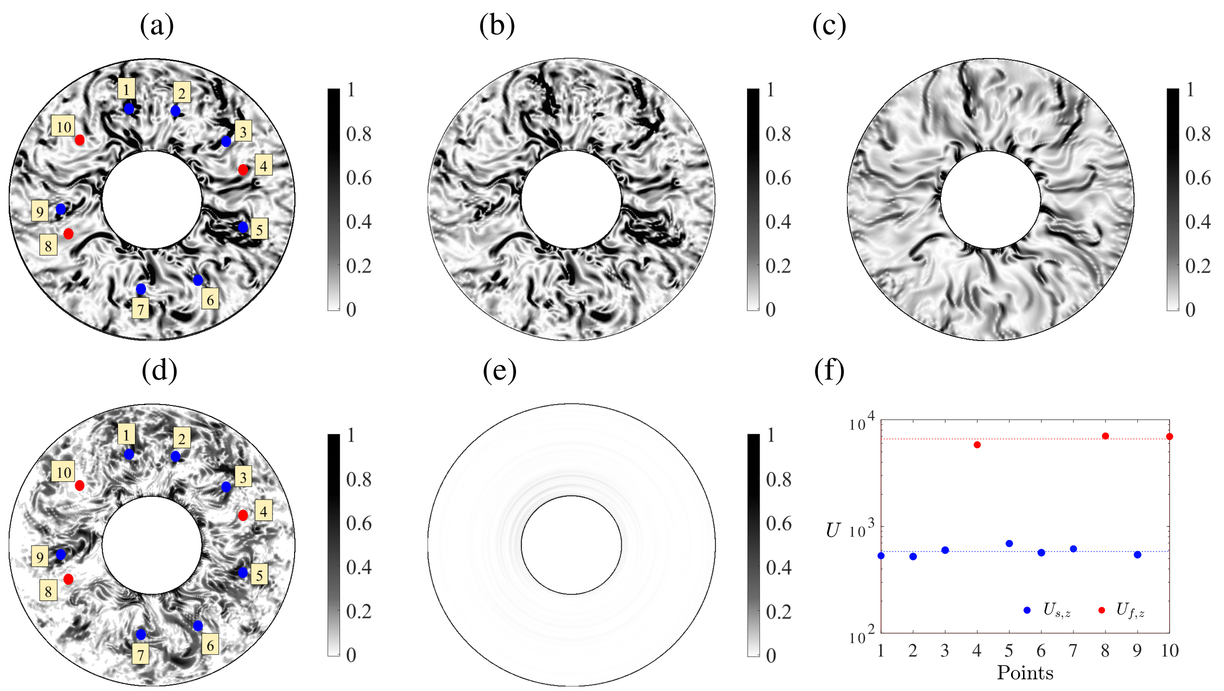

Figure S2: Greyscale plots on a horizontal section at $z = 0.2$ below the equatorial plane at the instant 'B' in figure S1, showing the ratio of the magnitudes of (a) Coriolis, (b) Lorentz, (c) buoyancy, (d) non-dipolar Lorentz, and (e) dipolar Lorentz force terms in the z-vorticity equation to the magnitude of the largest force among them. (f) The estimated (lines) and measured group velocities (points) for the blue and red points shown for figure (d). Here, $U_{f,z}$ and $U_{s,z}$ denote the measured axial group velocities of the fast and slow MAC waves, respectively. The dynamo parameters are $E = 1.2 \times 10^{-5}$, $Ra = 5000$, and $Pm = Pr = 1$.

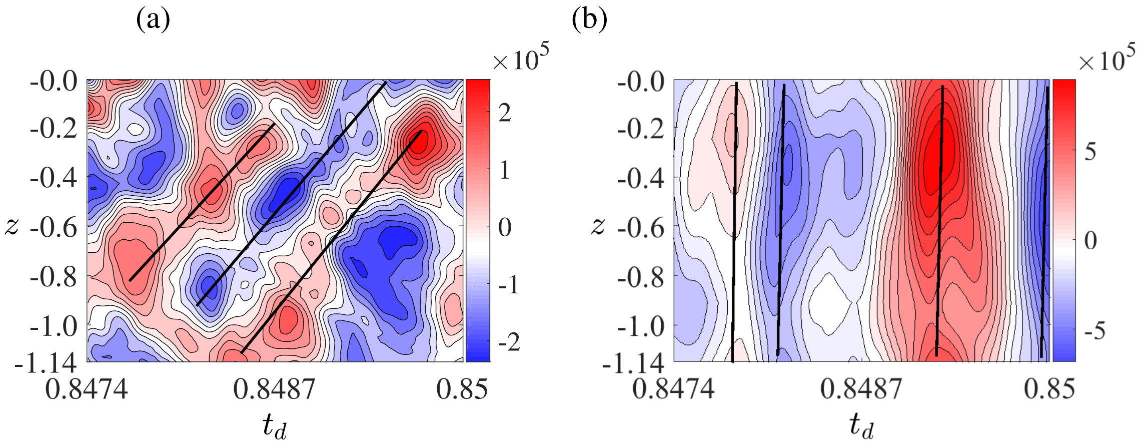

Figure S3: (a) & (b) Contour plots of $\partial u_z / \partial t$ at a cylindrical radius $s = 1$ for $l \leq l_E$ presented for the instant 'B' at points '1' and '4' respectively in figure S2(d). The parallel black lines indicate the primary wave travel direction, with their slopes denoting the group velocity. Panel (a) shows the propagation of slow MAC waves, whereas panels (b) show the propagation of fast MAC waves. The dynamo parameters are $E = 1.2 \times 10^{-5}$, $Ra = 5000$, $Pm = Pr = 1$.

polar (Sreenivasan & Kar, 2018), which indicates the essential role of the slow MAC waves in dipole formation.

S2 Mean resultant temperature gradient, β

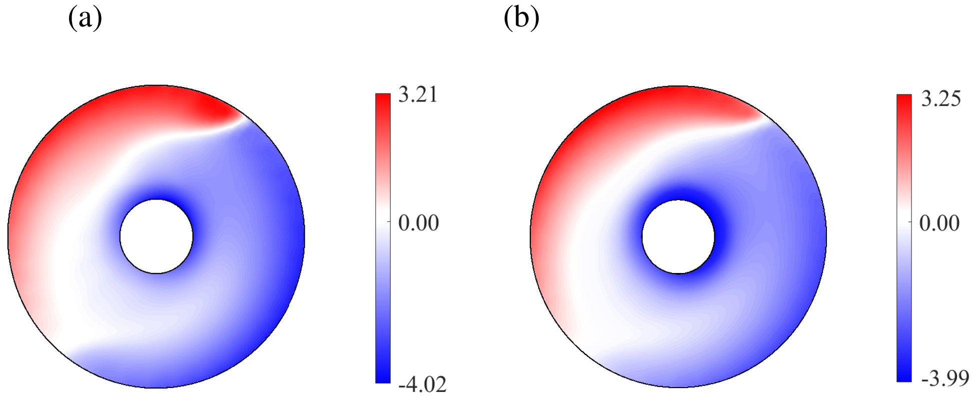

Figure S4: Horizontal section plots of the resultant temperature gradient β at $z = 0.4$ below the equator for (a) $Ra_V = 30$ (slightly below onset) and (b) $Ra_V = 310$ ($Ra_V/Ra_{V,c} \approx 10$) at $q^\star = 18$. A time average of ≈ 1 magnetic diffusion time is taken for the supercritical state to eliminate the effect of the perturbations in the convective state. The Y_2^1 heat flux heterogeneity is applied at the outer boundary. The other dynamo parameters are $E = 1.2 \times 10^{-5}$ and $Pm = Pr = 1$.

References

MAJUMDER, D., SREENIVASAN, B. & MAURYA, G. 2024 Self-similarity of the dipole–multipole transition in rapidly rotating dynamos. *J. Fluid Mech.* **980**, A30.

SREENIVASAN, B. & KAR, S. 2018 Scale dependence of kinetic helicity and selection of the axial dipole in rapidly rotating dynamos. *Phys. Rev. Fluids* **3** (9), 093801.

VARMA, A. & SREENIVASAN, B. 2022 The role of slow magnetostrophic waves in the formation of the axial dipole in planetary dynamos. *Phys. Earth Planet. Inter.* **333**, 106944.